

Tailoring the time response of a Bragg reflection to short X-ray pulses

W. Graeff

Hamburger Synchrotronstrahlungslabor HASYLAB am Deutschen Elektronen-Synchrotron (DESY), Notkestrasse 85, 22603 Hamburg, Germany. E-mail: walter.graeff@desy.de

The rather complicated time response of a crystal reflection to short incident pulses has been investigated by several authors. In this paper schemes are given to simplify this time response. In the Bragg case a small enough crystal thickness shortens the response considerably. In the Laue case the use of two successive reflections is very promising.

Keywords: free-electron lasers; X-ray optics; ultrashort X-ray pulses; dynamical diffraction.

1. Introduction

The free-electron laser (FEL) in the self-amplified spontaneous-emission (SASE) mode is a very promising tool for providing X-ray pulses with hitherto unprecedented high spectral brightness. Two projects are underway which promise to deliver these X-rays, namely the TESLA project at DESY (DESY, 1997, 2001, 2002) and the LCLS project at SLAC (SLAC, 1998). Impressive results have been obtained at the TESLA Test Facility (TTF) producing photon pulses of 100 nm wavelength with a pulse duration of 50–100 fs and a peak power of almost 1 GW (Ayvazyan *et al.*, 2002). A SASE FEL produces within 100–200 fs pulses with about 100 different modes resulting in a substructure of single spikes of duration 0.1 fs. Recently, however, a scheme has been proposed to produce single X-ray spikes of duration 100 attoseconds (Saldin *et al.*, 2002). In the past several authors have investigated the time response of crystals upon which such short pulses are incident.

The results differ for the two reflection geometries. In the Bragg case the reflected beam leaves the crystal on the same side as the incident beam, whereas in the Laue case it reflects off the back surface.

In the Bragg case, as calculated by Shastri *et al.* (2001a,b), a direct surface-reflected pulse occurs which has a characteristic width controlled by the strength of the reflection in use. Even for an incident pulse of duration a fraction of a femtosecond the response is several femtoseconds long. If the crystal is thin enough it is followed by a second peak, which is due to the 'echo' from the back surface of the crystal. This pulse is much shorter and several oscillations are visible afterwards. Its distance to the first peak is controlled by the crystal thickness. If the crystal is thick enough this peak vanishes due to absorption. Fig. 1 shows an example for the diamond 111 reflection. Diamond has been chosen because of its low absorption in view of the high intensity present in a FEL beam. The lowest possible reflection, which is 111 in diamond, has been considered to obtain an energy band as large as possible.

In the Laue case, between two prominent peaks the intensity oscillates as known from Pendellösung fringes (see Shastri *et al.*, 2001a; Graeff, 2002; Malgrange & Graeff, 2003).

The width of the interval between these two peaks depends on the crystal thickness. An example can be found in Fig. 5. Here an intrinsic width connected to the reflected energy range is not visible because the oscillations owing to the internal wavefields with slightly different wavenumbers dominate.

In both cases (Bragg and Laue case) the time response is obviously rather complicated. There is an intrinsic width of the reflected pulse which cannot be shortened even by using shorter incident pulses. The aim of this paper is to demonstrate that in both geometrical cases measures can be taken to shorten and simplify the time response considerably.

After initial submission the author was informed by the referee that the results in the Laue case were also independently obtained by Siddons (2001, 2004).

In view of the poorer quality of diamond (chosen to withstand the high heat load of a FEL beam) compared with silicon, the Bragg case is more likely to be used as a monochromator because a much smaller volume of the crystal is used in this case.

2. Description of ultrashort pulses

Usually ultrashort pulses are described by a δ function in time. This has the advantage that it leads to analytically solvable solutions (see *e.g.* Malgrange & Graeff, 2003). Therefore the frequency range of the incident pulse is unlimited.

In numerical simulations one has to introduce limits, usually dictated by the criterion that the result does not change within a certain tolerance. For short times after the onset of the reflected signal this requires a rather large range of the incidence parameter y . Therefore a stronger drop of the integrand would decrease the integration range. The assumption of a Gaussian input pulse produces such an effect and is in addition a more realistic model.

In the following simulations we assume as input an intensity pulse with a full width of 0.1 fs, the typical spike width within a SASE pulse. For a diamond 111 reflection this corresponds to $\sigma_y = 36.2$. The reflected wave is then obtained by using equations (10) and (10a),

$$I_R = \left| \int_{-\infty}^{\infty} G(y) R_{B,L}(y, T) \exp(2\pi i \beta y t) dy \right|^2, \quad (1)$$

with

$$G(y) = \exp(-y^2/2\sigma_y^2), \quad (2)$$

and the conversion factor β (8.79×10^{13} Hz) between the frequency ν and the incidence parameter y can be found from equation (8).

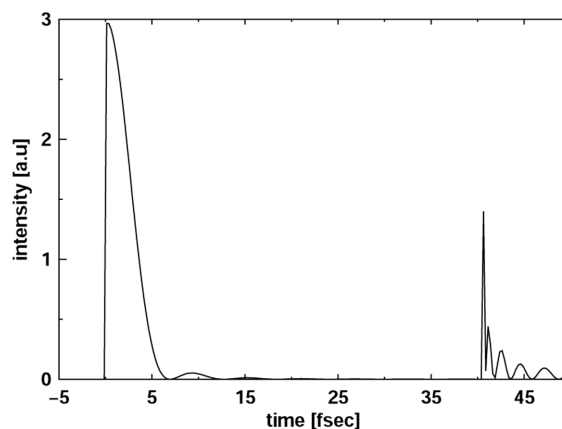


Figure 1

Time response of a diamond crystal of thickness $25 \mu\text{m}$ to a very short pulse with a central wavelength of 1 \AA , in the symmetric Bragg case. The 'echo' at 40 fs is due to the back surface. The abscissa shows the time in femtoseconds, and the ordinate shows the reflected intensity in arbitrary units.

3. Bragg reflection by thin crystals

With techniques developed in modern electronic device manufacturing, crystals can be made very thin. Also, thin crystalline films on substrates are feasible (see Appendix B). Therefore it makes sense to look at the response of an ultrathin crystal to a short X-ray pulse. Fig. 2 shows the result. For a variety of crystal thicknesses T the reflected intensities are plotted *versus* time. Whereas the surface-reflected intensity stays constant, the echo from the back surface moves towards the direct signal, as expected, but also changes its peak reflectivity drastically.

Above a certain thickness, the direct surface-reflected pulse is a function of the strength of the reflection in use. To give a rough estimate of its width we consider the total reflection range as being responsible for the time duration of the signal. The frequency range of a collimated beam can be estimated as

$$\Delta\nu_{\text{TR}} = \frac{c|\chi_h|}{\lambda \sin^2 \Theta_B} \quad (3)$$

using equation (8) and keeping in mind that the total reflection range is given by $|y| < 1$. The Fourier transform of such a frequency range is proportional to the function

$$\frac{\sin \pi \Delta\nu_{\text{TR}} t}{t} \quad (4)$$

Now the time duration of the intensity response at half-maximum can be obtained by the condition

$$\left[\frac{\sin \pi \Delta\nu_{\text{TR}} (\Delta t_{\text{TR}}/2)}{\Delta t_{\text{TR}}/2} \right]^2 = (\pi \Delta\nu_{\text{TR}})^2/2. \quad (5)$$

Solving the above equation yields, with the help of equation (3),

$$\Delta t_{\text{TR}} = 2.78 \frac{\lambda \sin^2 \Theta_B}{\pi c |\chi_h|}, \quad (6)$$

giving $\Delta t_{\text{TR}} = 5$ fs for the diamond 111 reflection, whereas the Fourier transform including the side tails gives 2.7 fs.

For very thin crystals of the order of a fraction of the extinction length ($\Delta_B = 7 \mu\text{m}$, $T = \Delta_B/\pi$, see Appendix A) the echo is no longer visible as a separate pulse but the surface-reflected intensity drops to zero. Obviously the echo is completely out of phase and cancels the surface reflection. In order to prove this, the surface-reflected wave and echo are calculated separately and compared with each other. The formulae are given in Appendix B. For two different crystal thicknesses the situation is illustrated in Fig. 3. The modulus of the amplitudes is shown *versus* time. The solid (positive) curve is the surface-reflected pulse and the dashed (for clarity negative) curve represents the part reflected from the back. Note that the onset of the surface-reflected part occurs immediately, as expected, whereas the back-reflected part starts with a delay, which depends on the thickness of the crystal, or, in other words, on the additional path the back-reflected part has to travel. Therefore, causality (the response comes after the excitation) is fulfilled using the side tails as well, both for the direct reflection and the ‘echo’. This is in contrast with the assumption that the total reflection range is responsible for the time response

solely, where the Fourier transform extends to negative times too. In other words part of the reflection occurs prior to the incident pulse.

For small crystal thickness T [case (b) of Fig. 3] the surface-reflected pulse and the echo can overlap in time significantly. For larger T [case (a) of Fig. 3] both waves no longer overlap in time but the echo is still modulated with varying thickness as can be seen in Fig. 2.

The reflected energy range increases when the crystal thickness becomes smaller than the extinction length. This is the region of the kinematical case. By making the crystal thinner and thinner, the accepted energy range even exceeds that of the incoming pulse and the reflected intensity drops to zero. Then it no longer makes any sense to call the crystal a monochromator.

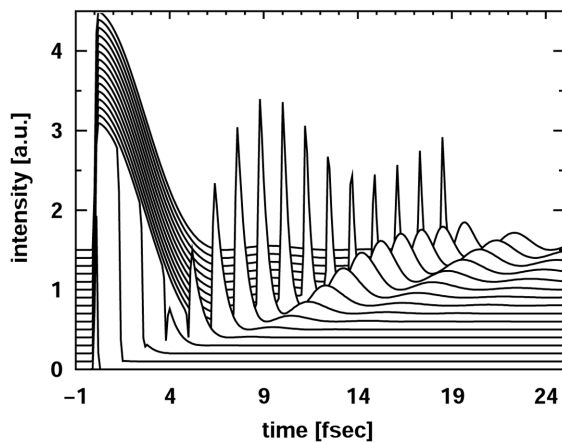


Figure 2 Intensity response of Bragg crystals (diamond 111) of different thickness *versus* time. The units of the abscissa are femtoseconds, whereas the ordinate is in arbitrary units. The crystal thickness for the first curve is $T = 0.1 \mu\text{m}$ and the thickness increases by $0.75 \mu\text{m}$ from curve to curve. Note that the curves are shifted by 0.1 arbitrary units in the vertical direction with respect to their neighbours for clarity (see text).

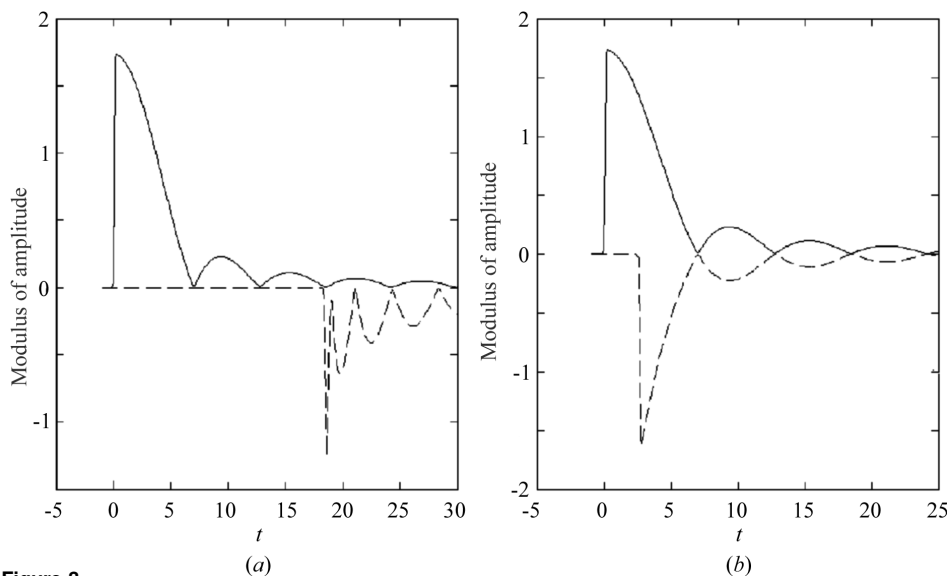


Figure 3 Modulus of amplitude. Solid (positive) curve: time response of surface-reflected pulse. Negative (dashed) curve: pulse reflected from the back surface. (a) $T = 11.35 \mu\text{m}$, which corresponds to the last curve of Fig. 2. (b) $T = 1.6 \mu\text{m}$, corresponding to the third curve of Fig. 2 (see text).

4. Laue reflection of two successive crystals

The focusing of wavefields at the exit surface when using two successive Laue reflections with crystals of equal thickness is well known (Fig. 4). Hence it is no surprise that from the rather complicated time structure after one Laue reflection (Graeff, 2002; Malgrange & Graeff, 2003) only the central peak is left after two reflections. As we assume an exact parallel setting of the two subsequent crystals ($y_1 = y_2$) we obtain the reflected plane waves after two reflections simply by taking the product of the amplitude ratios after one reflection (equation 10a) and integrating over y . Fig. 5 shows the intensity after one and two Laue reflections *versus* time. The intensity after one reflection shows a strong oscillatory behaviour and is dominated by two peaks at the margins. The distance of these two peaks is proportional to the thickness of the crystal. However, after a second reflection a single peak is left and the intensity around that peak is negligible and even drops to zero outside a region twice as wide as that of a single crystal. So the total duration of the signal is nominally doubled but only the central peak is significant. The total reflectivity can be maximized by varying the thickness of the crystal. A maximum in the vicinity of 100 μm occurs at 94.5 μm . A typical value of the width of the central peak for diamond 111, at 1 \AA , and with a crystal thickness of 94.5 μm is 1.7 fs, which is considerably smaller than the direct pulse in the Bragg case (2.7 fs).

In the case where large high-quality crystals are not available, the simple parallel setting of connecting the two Laue crystals *via* a common base is not possible. It is therefore interesting to determine the accuracy required to set the crystals parallel.

Owing to the oscillatory structure of the single-reflection curve in the Laue case, the rocking curve of two subsequent Laue-case crystals of equal thickness T shows a pronounced and narrow peak in the centre for certain values of T (Bonse *et al.*, 1977). A similar behaviour is seen when looking at the time response of two Laue crystals. The central peak requires a parallel setting of the two crystals within a very narrow angular range as seen from Fig. 6. Whereas the rocking curve has a full width at half-maximum of more than $\Delta y = 3$, the central peak in the time response is visible in a range of $\Delta y = 0.24$ only.

We may conclude that although the time response of a crystal reflection to an incident X-ray pulse seems to be rather complicated,

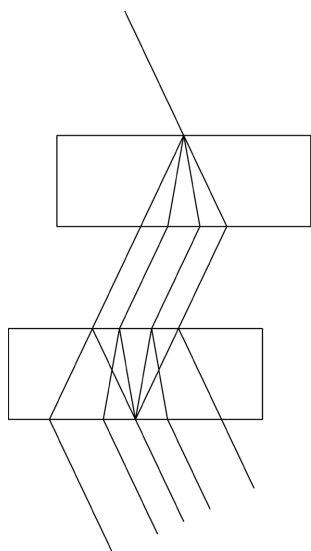


Figure 4
Focusing of wavefields when using two successive Laue crystals of equal thickness.

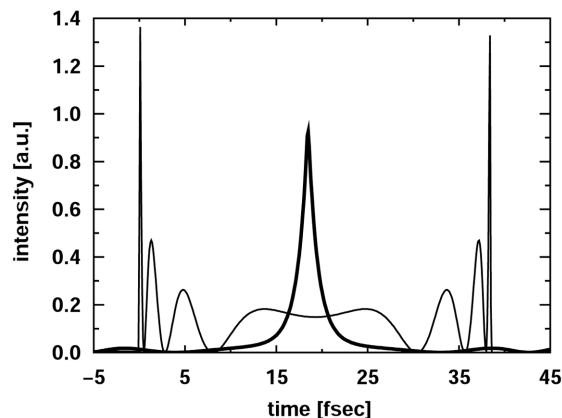


Figure 5
Time response of a single (thin line) and a double (thick line) Laue crystal (diamond 111 reflection, 1 \AA wavelength, 94.5 μm thickness). Whereas with a single Laue crystal the time response lasts for about 38 fs and is rather complicated, the non-dispersive reflection by a second Laue crystal of equal thickness is mainly a single spike, which sits on a very low-level intensity spread over an interval of 76 fs. For better visibility the central spike has been shifted by 20 fs; otherwise it would overlap with the second spike of the single reflection.

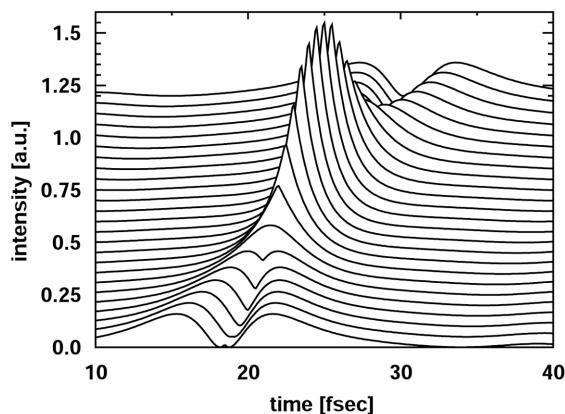


Figure 6
Time response of two non-dispersive Laue crystals with changing relative angle (rocking curve). Each line differs by $\Delta y = 0.025$ on the rocking curve. As the lines have been shifted in both x and y position, the origin is arbitrary.

there are ways of influencing the time structure. In the Bragg case the ‘echo’ is eliminated and the pulse width shortened considerably by making the crystal thinner. In the Laue case the two spikes, the distance of which even depends on the crystal thickness, can be turned into a single spike by two successive reflections.

APPENDIX A Some formulae from dynamical diffraction

For simplicity we restrict ourselves to centrosymmetric crystals ($\chi_h = \chi_{\bar{h}}$), linearly polarized light ($C = 1$) and the symmetric case. Formulae for the dynamical theory of X-ray diffraction have been given by numerous authors. We start from the formulae given by Bonse & Graeff (1977). The normalized incidence parameter y is given by

$$y = - \frac{\Delta\Theta \sin 2\Theta_B + (\chi_0)}{|\chi_h|}, \quad (7)$$

with $\Delta\Theta$ measuring the deviation from the exact Bragg angle Θ_B , and χ_m ($m = 0, h$) denoting the Fourier coefficients of the dielectric

susceptibility for different directions (complex values with absorption). The brackets in the numerator indicate that in the symmetric Laue case a refractive correction does not occur. Instead of the angular dependence of the incidence parameter, for our purpose the frequency dependence for a collimated beam is more adequate,

$$y = \frac{2\lambda \sin^2 \Theta_B}{c|\chi_h|} \Delta\nu = \frac{\Delta\nu}{\beta}, \quad (8)$$

where c/λ denotes the central frequency. An important quantity for the characterization of a reflection is the extinction distance for the Bragg case,

$$\Delta_B = \frac{\sin \Theta_B}{k|\chi_h|}, \quad (9)$$

and the Pendellösung length for the Laue case,

$$\Delta_L = \frac{\cos \Theta_B}{k|\chi_h|}, \quad (9a)$$

where k is as usual the wavenumber. Typical values for a diamond 111 reflection and 1 Å wavelength are $\Delta_B = 7.01 \mu\text{m}$ and $\Delta_L = 27.95 \mu\text{m}$. With the abbreviations $A = \pi T/\Delta_{L,B}$ (where T is the crystal thickness) and $\alpha = \chi_h/|\chi_h|$, we obtain for the amplitude ratio between reflected and incident wave for the Bragg case

$$E_h^e/E_0^i = R_B(y, T) = i\alpha \frac{S(y, T)}{C(y, T) + iyS(y, T)} \exp\left[-2\pi iz \left(\frac{k\chi_0}{\sin \Theta_B} + \frac{y}{\Delta_B}\right)\right], \quad (10)$$

and for the Laue case

$$E_h^e/E_0^i = R_L(y, T) = i\alpha S(y, T) \exp\left[\pi iT \left(\frac{k\chi_0}{\cos \Theta_B} + \frac{y}{\Delta_L}\right) + 2\pi iz \frac{y}{\Delta_L}\right], \quad (10a)$$

where

$$C(y, T) = \cos\left[A(y^2 \pm \alpha^2)^{1/2}\right], \quad (11)$$

$$S(y, T) = \frac{\sin\left[A(y^2 \pm \alpha^2)^{1/2}\right]}{(y^2 \pm \alpha^2)^{1/2}},$$

with the + sign for the Laue case and the – sign for the Bragg case. z measures the normal distance between the source (the origin) and the entrance face of the crystal.

Because the dispersion relation for the frequency ν and the wavenumber k is linear for X-rays outside regions of anomalous dispersion, the Fourier transforms in the spatial domain (spherical wave) and the time domain (short pulse) are similar† in shape, as shown in Fig. 7.

APPENDIX B Reflection from a crystalline layer on a substrate

It is shown that the reflection from a crystalline layer on a substrate in contrast to usual optics leads to the same expression for the reflected amplitude as known for the case when on both sides of the crystal is a vacuum.

Before we show that a refractive index different from 1 on the back surface (a substrate) makes no difference at least for the amplitude, let us calculate the surface-reflected wave separately to see its interference with the back-reflected wave more clearly. This is with a

† ‘Similar’ in the rigorous mathematical sense: equal disregarding a gauge factor.

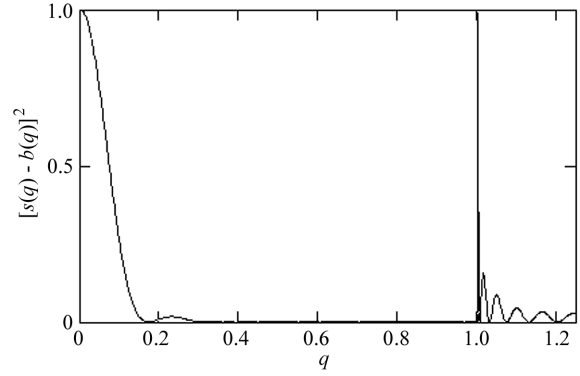


Figure 7

Spatial Fourier transform of an incident spherical wave as given by Saka *et al.* (1973). Crystal thickness and reflection parameters are the same as in Fig. 1. The surface-reflected wave is given by $s(q) = J_0(2Aq) + J_2(2Aq)$ and, neglecting absorption, the first back-reflected contribution by $b(q) = J_0[2A(q^2 - 1)^{1/2}] + 2[(q - 1)/(q + 1)] J_2[2A(q^2 - 1)^{1/2}] + \{[(q - 1)/(q + 1)]^2 \times J_4[2A(q^2 - 1)^{1/2}]\}$. q is a normalized spatial coordinate, J_n are Bessel functions. In reality, with absorption the echo, of course, would be smaller than the direct pulse. Note the similarity to Fig. 1, taking absorption into account, which mainly affects the echo.

transversely unbound plane wave somewhat artificial, but mathematically allowed because of the superposition principle. The incident plane wave is

$$E_0^i \exp[2\pi i(\mathbf{K}_0 \mathbf{r} - \nu t)]. \quad (12)$$

From now on we omit the time dependence for convenience of writing. The boundary condition at the entrance surface for the directly reflected beam, denoted $E_h^{e,s}$, requires that in the Bragg case only one wavefield is excited (usually numbered 2). The vector \mathbf{r}_e ends on the entrance surface. As usual, vacuum wavevectors are denoted \mathbf{K}_n whereas wavevectors inside the crystal are denoted $\mathbf{k}_n^{(j)}$, $j = 1, 2$, $n = 0, h$.

$$E_0^i \exp(2\pi i \mathbf{K}_0 \mathbf{r}_e) = E_0^{(2)} \exp[2\pi i \mathbf{k}_0^{(2)} \mathbf{r}_e], \quad (13)$$

$$E_h^{e,s} \exp(2\pi i \mathbf{K}_h \mathbf{r}_e) = E_h^{(2)} \exp[2\pi i \mathbf{k}_h^{(2)} \mathbf{r}_e].$$

A considerable amount of writing is avoided by the introduction of the following abbreviations,

$$k\delta_0^{(j)} = [\mathbf{K}_0 - \mathbf{k}_0^{(j)}] \mathbf{n},$$

$$k\delta_h^{(j)} = [\mathbf{K}_h - \mathbf{k}_h^{(j)}] \mathbf{n}, \quad (14)$$

$$P(x) = \exp(-2\pi i k x),$$

$$\xi^{(j)} = E_h^{(j)}/E_0^{(j)},$$

$$\mathbf{n} \mathbf{r}_e = z,$$

and by going to matrix notation,

$$\begin{pmatrix} E_0^i \\ 0 \end{pmatrix} = \begin{pmatrix} P[\delta_0^{(2)} z] & 0 \\ \xi^{(2)} P[\delta_h^{(2)} z] & -1 \end{pmatrix} \begin{pmatrix} E_0^{(2)} \\ E_h^{e,s} \end{pmatrix}. \quad (15)$$

The solution for the second unknown is

$$E_h^{e,s} = \xi^{(2)} E_0^i P\left[\left[\delta_h^{(2)} - \delta_0^{(2)}\right] z\right]. \quad (16)$$

From dynamical theory we know

$$\begin{aligned}
 2k\delta_0^{(1,2)} &= -\frac{k\chi_0}{\sin\Theta_B} - \frac{y \pm (y^2 - \alpha^2)^{1/2}}{\Delta_B}, \\
 2k\delta_h^{(1,2)} &= \frac{k\chi_0}{\sin\Theta_B} - \frac{-y \pm (y^2 - \alpha^2)^{1/2}}{\Delta_B}, \\
 \xi^{(1,2)} &= \frac{1}{\alpha} \left[y \pm (y^2 - \alpha^2)^{1/2} \right].
 \end{aligned} \quad (17)$$

Hence we obtain for the surface-reflected beam,

$$E_h^{e,s} = \frac{1}{\alpha} \left[y - (y^2 - \alpha^2)^{1/2} \right] \exp \left\{ -2\pi iz \left[\frac{k\chi_0}{\sin\Theta_B} + \frac{y}{\Delta_B} \right] \right\}. \quad (18)$$

Including the effect of the back surface requires rewriting the boundary conditions. On the back surface we allow for a substrate and assume a different refractive index than on the entrance side, expressed by wavevectors \mathbf{K}_n^b . A vector on the back surface is denoted by \mathbf{r}_b , where the relation $\mathbf{r}_b = \mathbf{r}_s + T\mathbf{n}$ holds (where \mathbf{n} is the surface normal).

$$\begin{aligned}
 E_0^i \exp[2\pi i \mathbf{K}_0 \mathbf{r}_e] &= E_0^{(1)} \exp[2\pi i \mathbf{k}_0^{(1)} \mathbf{r}_e] + E_0^{(2)} \exp[2\pi i \mathbf{k}_0^{(2)} \mathbf{r}_e], \\
 E_h^e \exp[2\pi i \mathbf{K}_h \mathbf{r}_e] &= E_h^{(1)} \exp[2\pi i \mathbf{k}_h^{(1)} \mathbf{r}_e] + E_h^{(2)} \exp[2\pi i \mathbf{k}_h^{(2)} \mathbf{r}_e], \\
 E_0^e \exp[2\pi i \mathbf{K}_0^b \mathbf{r}_e] &= E_0^{(1)} \exp[2\pi i \mathbf{k}_0^{(1)} \mathbf{r}_b] + E_0^{(2)} \exp[2\pi i \mathbf{k}_0^{(2)} \mathbf{r}_b], \\
 0 &= E_h^{(1)} \exp[2\pi i \mathbf{k}_0^{(1)} \mathbf{r}_b] + E_h^{(2)} \exp[2\pi i \mathbf{k}_0^{(2)} \mathbf{r}_b].
 \end{aligned} \quad (19)$$

Analogue to the abbreviations above we define

$$\begin{aligned}
 k\delta_0^{b,(j)} &= \left[\mathbf{K}_0^b - \mathbf{k}_0^{(j)} \right] \mathbf{n}, \\
 \mathbf{n} \mathbf{r}_b &= z + T,
 \end{aligned} \quad (20)$$

and the corresponding matrix

$$\begin{pmatrix} E_0^i \\ 0 \\ 0 \\ 0 \end{pmatrix} = \begin{pmatrix} P[\delta_0^{(1)} z] & P[\delta_0^{(2)} z] & 0 & 0 \\ \xi^{(1)} P[\delta_h^{(1)} z] & \xi^{(2)} P[\delta_h^{(2)} z] & 0 & -1 \\ P[\delta_0^{b,(1)}(z+T)] & P[\delta_0^{b,(2)}(z+T)] & -1 & 0 \\ \xi^{(1)} P[\delta_h^{(1)}(z+T)] & \xi^{(2)} P[\delta_h^{(2)}(z+T)] & 0 & 0 \end{pmatrix} \begin{pmatrix} E_0^{(1)} \\ E_0^{(2)} \\ E_0^e \\ E_h^e \end{pmatrix}. \quad (21)$$

Note that owing to the absence of a h wave behind the crystal the refraction of the substrate enters the boundary condition in the third equation only. It follows directly from the boundary conditions that the substrate has no influence on the reflected amplitude. We could stop here but we give the explicit solution of the boundary conditions in matrix form.

Solving this system of linear equations for E_0^e and E_h^e requires the knowledge of three determinants,

$$\det = \xi^{(1)} P[\delta_h^{(1)} T] - \xi^{(2)} P[\delta_h^{(2)} T], \quad (22)$$

where we used, for the symmetric Bragg case, $P[(\delta_0^{(1)} + \delta_h^{(2)})z] = 1$,

$$\det_3 = E_0^i P \left[\frac{\chi_0 - \chi_0^b}{2i \sin\Theta_B} (z+T) \right] [\xi^{(1)} - \xi^{(2)}], \quad (23)$$

$$\det_4 = -E_0^i \xi^{(1)} \xi^{(2)} \left\{ P[\delta_h^{(1)} z + \delta_h^{(2)}(z+T)] - P[\delta_h^{(2)} z + \delta_h^{(1)}(z+T)] \right\}. \quad (24)$$

According to Cramer's rule we obtain for the outgoing beams,

$$E_0^e = \frac{\det_3}{\det} = E_0^i P \left[\frac{\chi_0 - \chi_0^b}{2i \sin\Theta_B} (z+T) \right] \frac{\xi^{(1)} - \xi^{(2)}}{\xi^{(1)} P[\delta_h^{(1)} T] - \xi^{(2)} P[\delta_h^{(2)} T]}, \quad (25)$$

$$E_h^e = \frac{\det_4}{\det} = E_0^i P \left\{ [\delta_h^{(1)} - \delta_h^{(2)}] z \right\} \frac{\xi^{(1)} \xi^{(2)} \left\{ P[\delta_h^{(1)} T] - P[\delta_h^{(2)} T] \right\}}{\xi^{(1)} P[\delta_h^{(1)} T] - \xi^{(2)} P[\delta_h^{(2)} T]}. \quad (26)$$

After some calculation we obtain, using (17),

$$\frac{E_0^e}{E_0^i} = \exp \left[i\pi k \frac{(\chi_0^b - \chi_0)z + \chi_0 T}{\sin\Theta_B} + i \frac{\pi T}{\Delta_B} y \right] \frac{1}{C(y, T) + iyS(y, T)}. \quad (27)$$

Comparing this result with the case without a substrate, the amplitude is the same (energy conservation) whereas a phase factor $\exp[i\pi k[(\chi_0^b - \chi_0)/(\sin\Theta_B)](z+T)]$ corrects for the different k vectors,

$$\frac{E_h^e}{E_0^i} = i\alpha \frac{S(y, T)}{C(y, T) + iyS(y, T)} \exp \left\{ -2\pi iz \left(\frac{k\chi_0}{\sin\Theta_B} + \frac{y}{\Delta_B} \right) \right\}, \quad (28)$$

which is equation (10). Subtracting (18) from (28) gives the part of the reflected amplitude solely passed over the back-surface reflection.

The author wishes to thank Horst Schulte-Schrepping for technical assistance with preparing the figures, and Cécile Malgrange for carefully reading the manuscript.

References

- Ayvazyan, V., Sandner, W. & Will, I. (2002). *Phys. Rev. Lett.* **88**, 104802-1-104802-4.
- Bonse, U. & Graeff, W. (1977). *X-ray and Neutron Interferometry in Topics of Applied Physics*, Vol. 22, edited by H.-J. Queisser, pp. 93-143. Berlin: Springer.
- Bonse, U., Graeff, W., Teworte, R. & Rauch, H. (1977). *Phys. Status Solidi A*, **43**, 487-492.
- DESY (1997). Report DESY 1997-048, ECFA 1997-182. DESY, Hamburg, Germany.
- DESY (2001). Report DESY 2001-011, ECFA 2001-209. DESY, Hamburg, Germany.
- DESY (2002). Report DESY 2002-167, ECFA 2002-09. DESY, Hamburg, Germany.
- Graeff, W. (2002). *J. Synchrotron Rad.* **9**, 82-85.
- Malgrange, C. & Graeff, W. (2003). *J. Synchrotron Rad.* **10**, 248-254.
- Saka, T., Katagawa, T. & Kato, N., (1973). *Acta Cryst.* **A29**, 192-200.
- Saldin, E. L., Schneidmiller, E. A. & Yurkov, M. V. (2002). *Opt. Commun.* **212**, 377-390.
- Shastri, S. D., Zambianchi, P. & Mills, D. M. (2001a). *Proc. SPIE*, **4143**, 69-77.
- Shastri, S. D., Zambianchi, P. & Mills, D. M. (2001b). *J. Synchrotron Rad.* **8**, 1131-1135.
- Siddons, D. P. (2001). NSLS Activity Report 2001, Science Highlights 2-125-2-128. NSLS, Brookhaven, NY, USA.
- Siddons, D. P. (2004). In *Proceedings of the Eighth International Conference on Synchrotron Radiation Instrumentation (SRI 2003)*. In the press.
- SLAC (1998). Report SLAC-R-521, UC-414 (1998). Stanford Linear Accelerator Center, CA 94025, USA.